Proceedings of NFSI & ICFBI 2007
Hangzhou, China, October 12-14, 2007

Evaluation of BOLD Sensitivity Using a Realistic MRI Simulator

Ali-Reza Mohammadi-Nejad[1], G.-Ali Hossein-Zadeh[1], and Hamid Soltanian-Zadeh[1,2]
[1]Control and Intelligent Processing Center of Excellence, School of ECE, Univ. of Tehran, Tehran, Iran,
[2]Medical Image Analysis Lab., Henry Ford Health System, Detroit, Michigan, USA
a.mohammadinejad@ece.ut.ac.ir, ghzadeh@ut.ac.ir, hszadeh@ut.ac.ir

***Abstract*-MRI simulation is a suitable method to evaluate and acquire understanding of the complex blood oxygenation level dependent (BOLD) effect. To study the observablity of BOLD signal, we extended a MRI simulator. This simulator is capable of complete modeling of object (tissue) and main field inhomogeneities. We made a digital phantom in which the magnitude of fractional oxygenation (*Y*), hematocrit (Hct) values in red blood cells, the diameter of vessels, and also the position of blood vessel within the voxel can be changed. Then we created echo planar imaging (EPI) images of the phantom under resting and activated states using the simulator. Resulting images were analyzed using cross-correlation and t-test analysis for activation detection. Then the effect of various parameters on the detection of BOLD is investigated. These parameters include fractional oxygenation, spatial extent of BOLD effect and the location of vessel inside voxel. This simulation study provides a basis for planning experiments aimed at BOLD contrast detection with EPI pulse sequence.**

I. INTRODUCTION

Despite the popularity of functional magnetic resonance imaging (fMRI) in neuroimaging studies, there are limited works that characterize the precise relationship between brain activity and the observed MR signal changes. Several models describing blood oxygenation level dependent (BOLD) effect in MR images have been published. The models of Weisskoff *et al.* [1], Yablonsky *et al*. [2], and Spees *et al.* [3] are particularly instructive in describing specific aspects of BOLD contrast.

The molecular structure of hemoglobin strongly depends on the existence of oxygen. This structural feature can define the magnetic properties of red blood cells. The blood hemoglobin contains iron, and it can be in an oxygenated or deoxygenated state. Oxygenated hemoglobin is diamagnetic, whereas deoxygenated hemoglobin is paramagnetic. Opposite behavior of oxygenated and deoxygenated blood is the basis of the BOLD effect [4]. Studies have shown that voxels containing a mixture of paramagnetic and diamagnetic tissues produce field inhomogeneity at the interfaces due to the local susceptibility differences. These inhomogeneities manifest themselves in MR T_2^*-weighted images.

Recently, Weisskoff *et al.* [1] evaluated the difference in the susceptibilities of fully deoxygenated blood and fully oxygenated blood. They showed that this difference is about 0.18 ppm. Silvennoinen *et al.* [5] studied nuclear magnetic resonance relaxation rate in the blood at 4.7 T, which provide reference values for *in vivo* modeling. Cano *et al.* [6] determined the magnetic susceptibility of deoxygenated human red blood cell by Monte Carlo computer simulation. Their model showed a very good agreement with experimental values. Spees *et al.* [3] determined relaxation parameters of blood and found a magnetic susceptibility difference of 0.264 ppm between fully deoxygenated and fully oxygenated red blood cells at 37°C, as determined independently by MR and superconducting quantum interference device (SQUID) measurement.

As we see, many investigations reported both magnetic properties and the influence of an external magnetic field on red blood cells. However, characterization of the signal response from different values of fractional oxygenation, Hct, volume of vessels, and also the position of blood vessel within the image voxel, has yet to be described. This evaluation can be systematically performed via an MR simulator. On the other hand, as a supplement to experiments which is performed via MRI scanner, numerical simulations of BOLD effect can provide additional insight into the fMRI signal origination. The MRI simulators are mostly based on the numerical solution of Bloch equations. Study of BOLD effect via a MRI simulator can be useful in the systematic evaluation of the effect of each blood parameter on the BOLD signal by keeping all other parameters constant without the need of costly experimental measurements.

Under the light of previous works that presented the magnetic susceptibility of the blood under resting and activation states, we are able to simulate the MR signal which is originated from an activated region in a simulated object (tissue). Then we can produce numerous images from the simulated tissue under resting and activated states. By analysis of these images we can investigate the minimum detectable BOLD effect, the minimum detectable spatial extent of BOLD, etc.

In Section 2, we will explain our simulation strategy. Section 3 includes the results of simulations. Conclusions are presented in the final section.

II. METHOD

In this study, we used an open source MRI simulator known as SIMRI [7] which was implemented using Microsoft Visual C++ 6.0 and it has many advantages over other MRI simulators. SIMRI includes an efficient T_2^* management which makes it suitable for studying the effects of field inhomogeneities. In addition to the main static field value, it accepts a 3-dimentional (3D) or 2D map of the field inhomogeneities [7]. Other inputs to

1-4244-0949-7/07/$25.00 ©2007 IEEE

Table 1. The T1, T2, Proton density and magnetic susceptibility values used for different tissue types (the Montreal data set [8]).

Tissue Type	*T1 (ms)*	*T2 (ms)*	ρ	$\chi \cdot 10^{-6}$
Air	0	0	0	0.00
CSF	2569	329	1	-9.05
Gray Matter	833	83	0.86	-9.05
White Matter	500	70	0.77	-9.05
Muscle	900	47	1	-9 to -10
Skin	2569	329	1	-9.05
Skull	0	0	0	-8.86
Fat	350	70	1	-7 to -8
Glial Matter	833	83	0.86	-9.05
Connective	500	70	0.77	-9.05

the SIMRI are the object definition, and a description of the acquisition protocol. The object definition includes the determination of object dimensions, voxel sizes, T_1, T_2, and spin density (ρ) values for each voxel. For our simulation purpose, we use a 2D object description.

The first stage of simulation is to make a virtual object as input. A 256×256 MRI image was segmented to white matter, gray matter, CSF, scalp, and air (Fig. 1.a), by a Fuzzy C-mean (FCM) algorithm. Appropriate relaxation and spin density parameters are assigned to these parts by simulator based on Table 1. The spatial resolution of the virtual object (model of tissue) was 1×1 mm^2. On the other hand, the spatial resolution of image which was determined by the pulse sequence was 4×4 mm^2. By this technique, each voxel of output image is the map of 4×4 sub-voxels. Thus, the virtual object's matrix size was 256×256, and the output image was 64×64. The static magnetic field (B_0) was 1.5 T.

We used a 2-shot echo planar imaging (EPI) pulse sequences which has been added to SIMRI in our previous work [9]. Other parameters of this pulse sequence were TR = 0.3 sec, and flip angle of 90°. In each simulated fMRI session, we produced 60 sequential images of the same slice of brain tissue (30 images in resting state, and 30 images in activation state).

To produce the 2D map of the field inhomogeneity (originated from brain activity) we used a primitive model of red blood cells which was proposed in previous works. Accordingly, blood vessels can be modeled as right circular cylinders of constant susceptibility. In reality, the changes in the magnetic field due to the presence of a cylinder to the applied field are given by 'ΔB_{out}' and 'ΔB_{in}' where the former represents the resultant field outside the cylinder and the latter describes the resultant field inside the cylinder [10-12].

$$\Delta B_{in}(\rho,\theta) = \frac{\Delta\chi}{6} B_0 \left(3\cos^2\theta - 1\right)$$
$$\Delta B_{out}(\rho,\theta) = \frac{\Delta\chi}{2} B_0 \left(\frac{\alpha}{\rho}\right)^2 \sin^2\theta.\cos 2\phi \quad (1)$$

In the above Eq., ρ is radius in cylindrical coordinate (ρ=0 is the cylinder axis), θ is the angle extended by the vein with respect to the filed, α is the radius of the vessel, ϕ is the polar angle in the x-y plane of the observation point given by $\mathrm{Tan}^{-1}(y/x)$, $\Delta\chi$ is the susceptibility shift given by χ_i-χ_o in the presence of a background tissue with 'χ_i' and 'χ_o' representing the susceptibility inside and outside the vessel and B_0 is the applied magnetic field. Susceptibility of the blood system in general is given by [3]:

$$\chi_{blood} = Hct(\chi_{oxy} + (1-Y)\chi_{deoxy}) + (1-Hct)\chi_{plasma} \quad (2)$$

where χ_{blood}, χ_{oxy}, χ_{deoxy}, and χ_{plasma} represents the magnetic susceptibilities of the whole blood, oxygenated blood, deoxygenated blood, and plasma, respectively [3]. *Hct* is the hematocrit (which is a function of blood vessel diameter, and it is approximately 0.4 in large vessels, and about 0.3 at the capillary level [3]), *Y* is the oxygenation level which describes the fractional oxygenation in red blood cells. The fractional saturation of hemoglobin is reduced from 0.97 (arterial side) to 0.59 (venous side) as blood passes through the capillary bed. In the simulations, we set *Y* = 0.5 for resting state, and different values between 0.55 and 0.95 for *Y* in the activated state (various activation levels) in active voxels.

Any change in the oxygenation level alters the susceptibility which can be represented as [11]:

$$\Delta\chi_{blood} = -\Delta Y(\chi_{deoxy} - \chi_{oxy})Hct \quad (3)$$

where 'χ_{deoxy}-χ_{oxy}' is the difference in susceptibility of fully deoxygenated blood and fully oxygenated blood. This term has been evaluated and set to 0.18 ppm by Weisskoff *et al.* [1] and 0.264 ppm more recently by Spees *et al.* [3]. In this study we used 0.264 ppm for it.

Empirically, normal tissue has approximately the same susceptibility as arterial blood, which means that 'χ_{oxy}' is equal to 'χ_{tissue}'. Therefore, (3) now becomes [10-12]

$$\Delta\chi_{blood,tissue} = \frac{4\pi}{3}(0.264)Hct(1-Y) \quad (4)$$

In this model, we assumed that vessel is parallel to the static magnetic field. Owing to its orientation, there exists no extra-vascular field effect. Therefore, the susceptibility of blood is linearly proportional to the fractional hemoglobin saturation, *(1-Y)*. Thus, the change in field inside the vessel, originated from neural activity, can be written as:

$$\Delta B = \frac{4\pi}{3}(0.264)B_0(1-Y)Hct \quad (5)$$

where, ΔB is the field difference between blood and the surrounding tissue.

Thus for simulating the activation state, we set the ΔB (the field inhomogeneity parameter in the simulator) for some predefined voxels of the object according to (5). The field inhomogeneity parameters for other voxels were similar to that of resting state. 10 EPI images are acquired under activation state and 10 images under resting state (TR=0.3 sec). This on-off period was repeated three times to generate a series of 60 images.

A zero-mean and white Gaussian noise is added to the real and imaginary parts of the echoes in the K-space, such that the standard deviation of noise was 0.26 times of the mean of K-space values. We then analyzed the resulting images for activation detection using the cross correlation and t-test methods.

Therefore by using the straightforward correlation method, we derived a *CC* value for each voxel via:

$$CC = \frac{\sum_{j=1}^{N}(x_j - \mu_x)(r_j - \mu_r)}{\left[\sum_{j=1}^{N}(x_j - \mu_x)^2\right]^{1/2}\cdot\left[\sum_{j=1}^{N}(r_j - \mu_r)^2\right]^{1/2}} \qquad (6)$$

here x_j, and r_j ($j = 1...N$) are the time-courses of (a given) voxel, and reference signal. The reference signal **r** was set to the stimulation pattern (box-car). Terms μ_x and μ_r are the average values of vectors **x** and **r**, respectively and *N* is the numbers of time points of experiment.

For performing the hypothesis test on the *CC* parameter, we converted it to *z* parameter by using Fisher transform via:

$$z = \frac{1}{2}\ln\frac{1+CC}{1-CC}. \qquad (7)$$

Under null hypothesis, *z* has a zero mean Gaussian distribution. Its standard deviation is estimated from resting voxels.

Also, for showing the effect of vessel diameter (volume) on the BOLD effect, we run the simulation for different vessel-volumes ranging from 4% to 36% by using t-test method. By using this method, we derived a *T* value for each voxel via:

$$T = \frac{\sum_{j=1}^{N}(x_j - \mu_x)\tilde{r}_j}{\left[\sum_{j=1}^{N}(x_j - \mu_x)^2 - \left(\sum_{j=1}^{N}(x_j - \mu_x)\tilde{r}_j\right)^2\right]^{1/2}} \qquad (8)$$

All of the parameters in this Eq. are the same as cross-correlation method, except $\tilde{\mathbf{r}}$, which is the reference signal that has zero mean and unit norm.

Since the fraction blood in a voxel may have different values, it is likely that the heterogeneity in the distribution of blood volume in each voxel is low for the small vessels and high for larger vessels. It can be assumed that capillary blood volume, is about 1/2 of the total voxel volume, and it is homogeneously distributed across voxels. For larger vessels, a single vessel may completely fill several voxels, giving a 100% blood volume.

We also changed the position of vessel within each voxel to see its effect on the resulted signal. It is noteworthy that our imaging voxel contains 16 sub-voxels in the object level which enables us to perform such studies. The position of the vessel

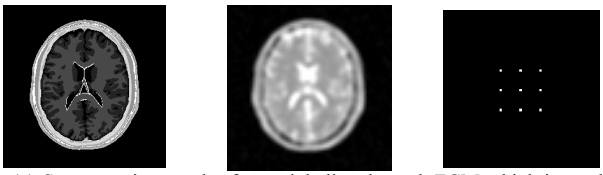

Fig.1. (a) Segmentation result of an axial slice through FCM which is used for building the object model for MR simulator. (b) An EPI image of the virtual object produced by MR simulator. (c) A map of activated voxels in the virtual object.

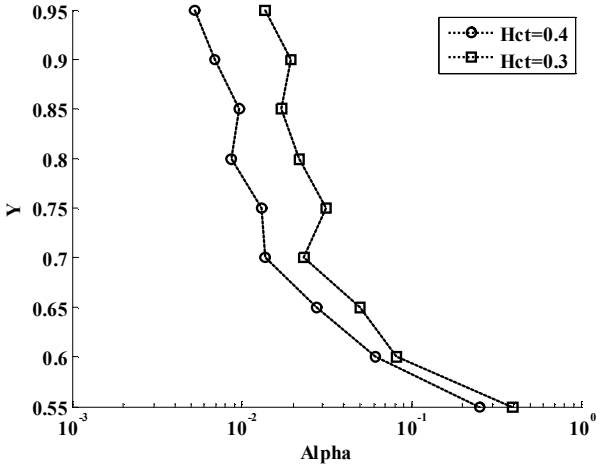

Fig.2. Minimum value of Y that is required for detecting the activity at each false alarm rate (Alpha) (for Hct = 0.3, and 0.4). Detection sensitivity decreases at lower alpha, and lower Hct's.

varied throughout the diameter of that voxel. For this experiment we placed our simulation vessel in sub-voxels 1, 6, 11 and 16, respectively. To study the effect of this position on the detection sensitivity we used receiver operating characteristic (ROC) curves. ROC method provides a standardized and statistically meaningful tool for comparing signal detection accuracy in various states/methods.

III. RESULTS

Several sets of simulated fMRI data were generated according to previous section and then analyzed for a systematic study on the detection sensitivity of BOLD effect.

After analysis of resulted fMRI images, we thresholded the resulting map of *z* values at different false alarm rates. Fig. 1.b shows a typical (simulated) EPI image of the slice, and Fig. 1.c shows detected activation areas for false alarm rate of 0.0066, that includes all activated areas with no false detection. For each amount of false alarm rate (or threshold) we determined the minimum *Y* that can be detected. Fig. 2 shows the resulted curve for two amounts of Hct's. As this figure illustrates, for higher amounts of specificities (lower alpha's) the minimum brain activity that can be detected considerably increases (Y increases). For example if we set the false alarm rate in the cross-correlation analysis less than 0.01 we cannot detect *Y*'s below 0.6, in Hct=0.4.

In the next study we evaluated the effect of spatial extent of BOLD effect (within the voxel) on the detection sensitivity of

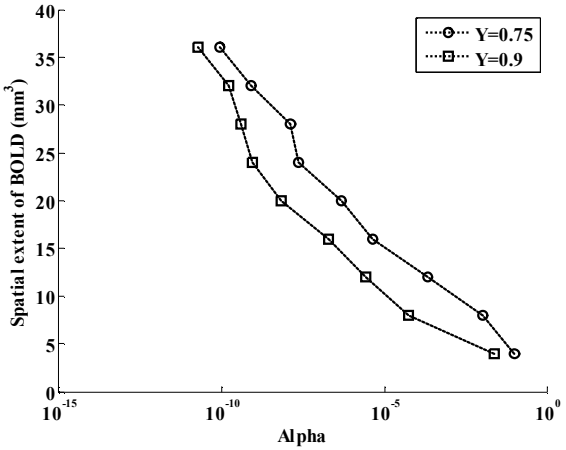

Fig.3. The minimum alpha required to detect each spatial extent of BOLD effect (for Hct=0.3 and Y = 0.9, and 0.75). By increasing the spatial extent of BOLD the minimum value of alpha is increased, which means that wider BOLD effects may be detected more easily.

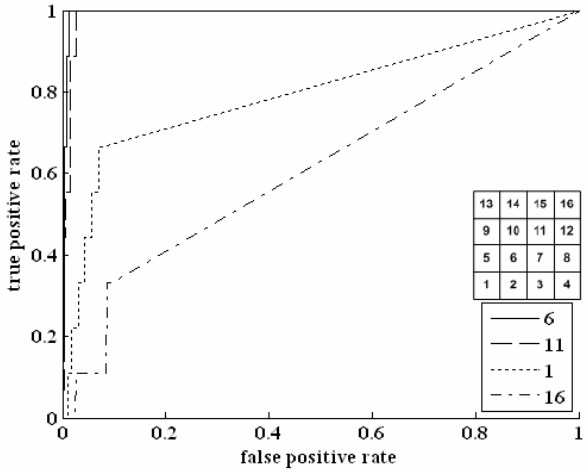

Fig.4. ROC curves for various positions of blood vessels within the image's voxel (Hct = 0.3 and Y = 0.4). Position of sub-voxels that contains the vessel is depicted in the small table.

BOLD. It is noteworthy that each image voxel include 16 sub-voxles in the object. In the previous results, we placed blood vessel in the central sub-voxel which is equal to considering only 1/16 of that voxel to be active. The results of changing the spatial extent of BOLD effect (increasing number of active sub-voxels within each imaging voxel) are reflected in Fig. 3. Fig. 3 shows, the minimum alpha required to detect activity at each spatial extent of BOLD. By increasing the spatial extent of BOLD the minimum value of alpha is increased, which means that wider BOLD effects may be detected more robust (at lower false alarm rates). Also, this figure shows that the vessels with large volume and high amount of activity (Y=0.90) can be detected more easily and robustly. T-test is used for this part of study.

Finally, we studied the effect of vessels position in the voxel. For this purpose, we changed the position of active sub-voxel across the voxel's diameter. The result of this experiment is shown in Fig. 4. As we see, by increasing the distance of active sub-voxel from the center of image voxel, the area under the ROC curve decreases. Thus, our detection accuracy is optimum for effects corresponding to the center of voxel.

IV. CONCLUSION

In this paper, we presented a tool for evaluating the effect of various parameters on the detection of BOLD, without the need of costly measurements. We used a primitive model to describe the effect of various parameters on the magnetic properties of human blood. Results of our simulation showed that the values of fractional hemoglobin, position of blood vessel within the voxel and also the occupied volume of voxel by blood vessel are very important factors in the accuracy of BOLD contrast detection.

REFERENCES

[1] R. Weisskoff and S. Kiihne, "MRI susceptometry: image-based measurement of absolute susceptibility of MR contrast agents and human blood," *Magn. Reson. Med*., Vol. 24, pp. 375–383, 1992.

[2] D. A. Yablonsky and E. M. Haacke, "Theory of NMR signal behavior in magnetically inhomogenous tissues: the static dephasing regime," *Magn. Reson. Med*, Vol. 32, pp. 749-763, 1994.

[3] W. M. Spees, D. A. Yablonskiy, M. C. Oswood and J. J. H. Ackerman, "Water proton MR properties of human blood at 1.5 Tesla: Magnetic susceptibility, T1, T2, T2*, and non- Lorentzian signal behavior," *Magnet. Reson. Med.*, Vol. 45, pp. 533-542, 1992.

[4] S. Ogawa, T. M. Lee, A. R. Kay and D. W. Tank, "Brain magnetic resonance imaging with contrast dependent on blood oxygenation," *Proc. Natl. Acad. Sci. U.S.A.*, Vol. 87, pp. 9868-9872, 1990.

[5] M. J. Silvennoinen, M. I. Kettunen, C. S. Clingman, and R. A. Kauppinen, "Blood NMR relaxation in the rotating frame: mechanistic implications," *Arch. Biochem. & Biophys*., Vol. 405, pp. 78–86, 2002.

[6] M. E. Cano, A. Gil-Villegas, M. A. Sosa, J. C. Villagomez and O. Baffa, "Computer simulation of magnetic properties of human blood," *Chem. Phys. Lett.*, Vol. 432, pp. 548–552, 2006.

[7] H. Benoit-Cattin, G. Collewet, B. Belaroussi, H. Saint- Jalmes and C. Odet, "The SIMRI project: a versatile and interactive MRI simulator," *J Magn Reson*, Vol. 173, Issue 1, pp. 97-115, 2005.

[8] D.L. Collins, A.P. Zijdenbos, V. Kollokian, J.G. Sled, N.J. Kabani, C.J. Holmes, and A.C. Evans, "Design and construction of a realistic digital brain phantom," *IEEE Trans. on Med. Imaging*, vol. 17, pp. 463-468, 1998.

[9] A. R. Mohammadi-Nejad and G. A. Hossein-Zadeh, "Simulation of echo planar imaging in MRI: application to assessment of field inhomogeneity and chemical shift, "*IEEE ISSPA '07 Conf.* , Sharjah, 12-15 Feb. 2007.

[10] M. Haacke, Y. Xu, Y. Cheng and J. Reichenbach, "Susceptibility weighted imaging", Magnet. Reson. Med., Vol. 52, pp. 612–618, 2004.

[11] M. Haacke, R. Brown, M. Thompson and R. Venkatesan, "Magnetic resonance imaging: physical principles and sequence design", *WILLEY-LISS Publication*, 1999.

[12] V. Seghal, Z. Delproposto, M. Haacke, K. Tong, N. Wycliffe, D. Kido, Y. Xu, J. Neelavalli, D. Haddar and J. Reichenbach, "Clinical applications of neuroimaging with susceptibility weighted imaging", *J. Magn. Reson. Imag.*, Vol. 22, pp. 439-450, 2005.